CHARACTERIZATION OF K-BAND RADIO FREQUENCY INTERFERENCE FROM AMSR-E, WINDSAT AND SSM/I

Darren McKague, John J. Puckett and Christopher Ruf

University of Michigan

ABSTRACT

An algorithm to detect radio-frequency interference in microwave radiometer brightness temperatures is developed and applied to K-band observations from AMSR-E, WindSat and SSM/I. This algorithm uses the monthly peak difference between co-polar brightness temperatures at 22 and 19 GHz to find RFI. Data from July 2005, July 2008, and January 2008 are shown. Less K-band RFI is seen in SSM/I data than in WindSat or AMSR-E data, likely due to differences in K-band center frequency and spatial resolution. A significant source of RFI is present in the 2008 and 2009 AMSR-E and WindSat data that was not present in 2005. This is likely due to transmissions from the DirecTV 10 satellite, which was launched in July of 2007. This RFI source is seen in reflection off of the Earth's surface. This reflection is strongest over ocean, but is also seen over snow where the diffuse component of the reflection creates a relatively wide swath of RFI.

Index Terms— microwave radiometry, radio-frequency interference

1. INTRODUCTION

Radio Frequency Interference (RFI) from human sources is a significant issue for passive microwave observations of the Earth. Numerous studies have shown the influence of RFI on Earth remote sensing in a number of bands including L [1], C [2, 3], and X [2, 3]. An understanding of the sources and frequency ranges of the RFI will help guide the design of future radiometers. To that end, this paper presents characteristics of K-band RFI over the continental US in two different frequency ranges, the first centered at 18.7 GHz, and the second centered at 19.35 GHz. The motivation is to provide guidance in the selection of K-band pass-bands for future radiometers For this, an algorithm for the detection of RFI was developed (Section 2) and applied to three different space-borne microwave radiometers with varying pass-bands (Section 3).

2. RFI DETECTION ALGORITHM

Based on the goal of providing general guidance rather than a quantitative analysis of RFI, a relatively simple algorithm for RFI detection was used. Data over the continental US were collected in ¼ degree latitude, longitude cells. In each of these cells, the maximum difference between co-polar brightness temperature (T_b) measurements at two relatively close frequencies for each instrument of interest were recorded for each month. Large negative or positive signals in these maximum differences generally result from either spectral variability in the geophysical signal or RFI in one of the two bands. By choosing co-polar bands that are close in frequency, the geophysical variability between bands can be minimized (though not entirely eliminated). The difference between geophysical variability and RFI can generally be identified by the magnitude and sign of the difference, as will be demonstrated in Section 3.

3. RFI CHARACTERIZATION

K-band data from the WindSat, Special Sensor Microwave Imager (SSM/I) F13 and Advanced Microwave Scanning Radiometer-EOS (AMSR-E) radiometers have been analyzed using the RFI detection algorithm described above. The center frequencies, bandwidths, polarizations, spatial resolutions, and incidence angles of the K-band channels around 19 GHz are shown in Table 1 for each instrument. Differences between the co-polar channels near 23 GHz were used for RFI detection. Data were analyzed for the periods July 2005 – June 2006 and July 2008 – June 2009.

Table 1. Relevant characteristics of K-band channels for WindSat, AMSR-E, and SSM/I.

Instrument	Center Frequency (GHz)	Bandwidth (MHz)	Polarization	Resolution (km)	Incidence Angle (degrees)
WindSat	18.7	500	V, H	27x16	55.35
AMSR-E	18.7	200	V, H	27x16	55
SSM/I	19.35	200	V, H	69x43	53.1

Selected T_b difference maps are shown in Figs. 1 through 8. Fig. 1 shows data from SSM/I, AMSR-E and WindSat from July 2005. Fig. 2 shows the same for July 2008, and Fig. 3 shows data from January 2009. Several features of note are seen in the data:

1. Large areas of positive and negative T_b differences are seen over the US. The positive differences are generally due to geophysical targets, such as open water and water vapor, or due to the spatial resolution mismatch between the two frequencies, as seen along the coasts for SSM/I. Some of the negative differences are from geolocation errors, like the features along coasts seen in AMSR-E, or from data quality issues, as seen for SSM/I over Texas in Fig. 3. The majority of the remaining negative differences are likely from RFI, since very few geophysical signals at these frequencies decrease with increasing frequency with the magnitude shown here (>15 K difference over <5 GHz).
2. SSM/I data show significantly less RFI than either AMSR-E or WindSat data. This is likely due to a combination of the lower resolution of SSM/I, and the fact that SSM/I has a different center frequency.
3. AMSR-E and WindSat show more RFI in 2008-2009 (Figs. 2, 3) than in 2005 (Fig. 1). This RFI is predominantly in an arc peaking around 45° North latitude centered at around 100° West longitude. The DirecTV 10 satellite, launched in 2007, is located in geosynchronous orbit with a sub-satellite point at around 100° West longitude. This satellite broadcasts from 18.3 to 18.9 GHz. Based on the relative positions of the satellites and incidence angles of the radiometers, specular reflection of the DirecTV signal would show up in AMSR-E and WindSat data in an arc peaking around 45° North latitude. This arc of RFI is therefore very likely due to DirecTV 10. Since the broadcasts don't overlap the SSM/I K-band channel, they should not and do not appear in the SSM/I observations.
4. The DirecTV RFI increases significantly over land in the winter (Fig. 3). This is likely due to increased reflection from snow, which has a higher reflectivity at these frequencies than bare or vegetated land surfaces. This signal also has a wider spatial extent than the RFI over water, which is likely due to the higher diffuse component of scattering from snow relative to water.
5. The DirecTV RFI over land is larger for AMSR-E than it is for WindSat (Figs. 2, 3). This could be due to the fact that the DirecTV broadcasts cover 100% of the AMSR-E pass-band while covering only 90% of the WindSat pass-band.

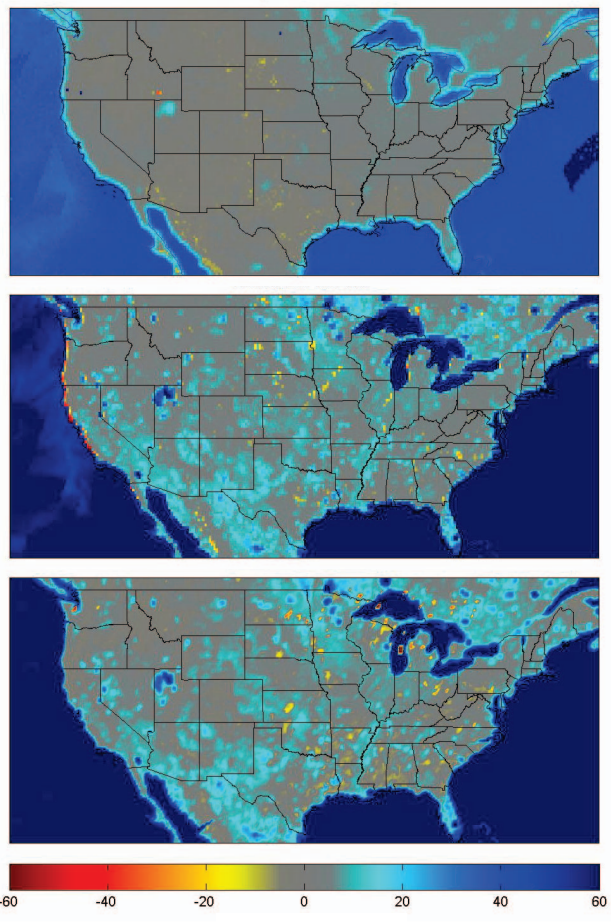

Figure 1. K-band RFI for SSM/I (top), WindSat (middle) and AMSR-E (bottom) for July 2005. Values shown are 22.235V – 19.25V Tb differences for SSM/I and 23.8V – 18.7V Tb differences for WindSat and AMSR-E. RFI appears as negative differences < 10 K (yellow through red).

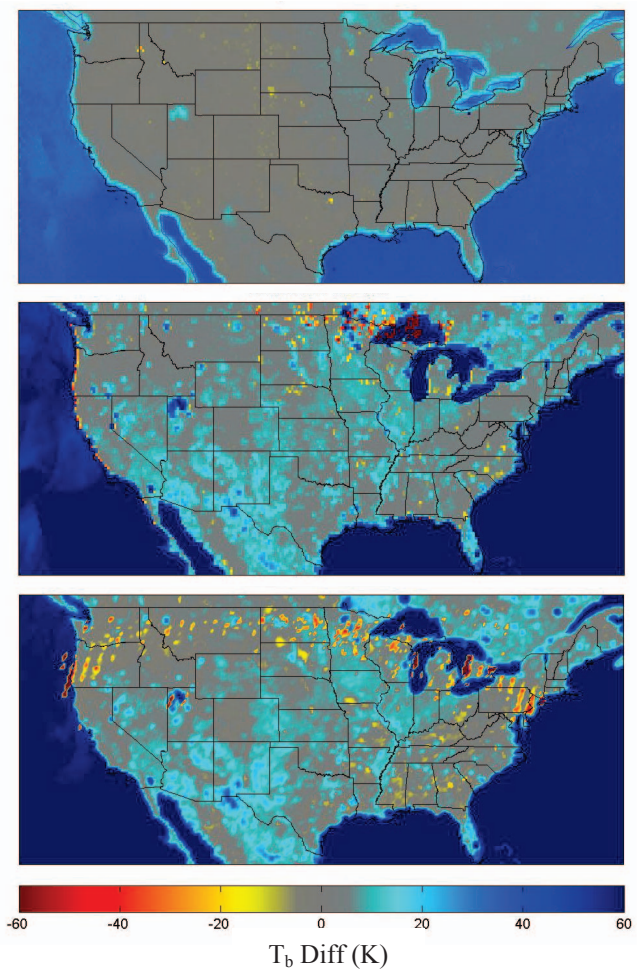

Figure 2. K-band RFI for SSM/I (top), WindSat (middle) and AMSR-E (bottom) for July 2008.

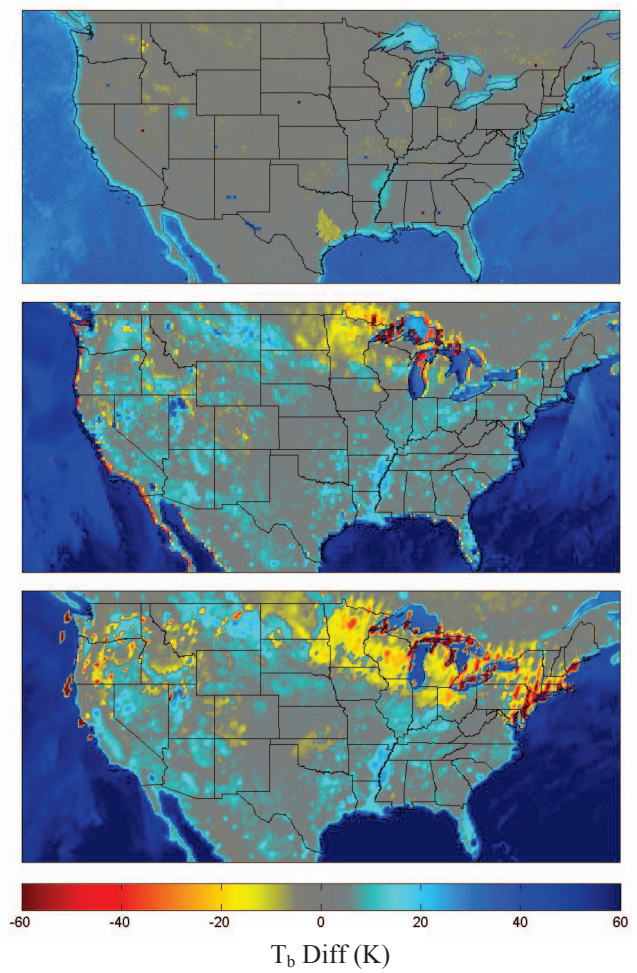

Figure 3. K-band RFI for SSM/I (top), WindSat (middle) and AMSR-E (Bottom) for January 2009.

3. CONCLUSIONS

An RFI detection algorithm has been used to look at the frequency dependence and spatial distribution of RFI at K-band for the AMSR-E, WindSat and SSM/I radiometers. The algorithm is based upon the maximum difference over a month between co-polar measurements at 19 and 22 GHz. Maps of RFI from the algorithm suggest that the SSM/I band, centered at 19.35 GHz, has less RFI over the US for the time period under study than do the AMSR-E and WindSat bands centered at 18.7 GHz. A broad arc of RFI across the northern US in AMSR-E and WindSat data has been traced to broadcasts from the DirecTV 10 satellite. This arc of RFI is highest in magnitude over water, though it shows significant spatial extent over land in the winter, most likely due to diffuse scattering from snow. Future investigations will consider if it is possible to use this signal to retrieve the snow water equivalent in the affected region.

11. REFERENCES

[1] Le Vine, D.M., "ESTAR experience with RFI at L-band and implications for future passive microwave remote sensing from space," *Geosci. Rem. Sens. Symposium*, 2002, vol. 2, pp. 847-849, 24-28 June 2002.

[2] Njoku, E.G., P. Ashcroft, T.K. Chan, and L. Li, "Global survey and statistics of radio-frequency interference in AMSR-E land observations," *IEEE Trans. Geosci. Rem. Sens.*, vol. 43, pp. 938-947, 2005.

[3] Li, Li, P.W. Gaiser, and M. Bettenhausen, "WindSat radio-frequency interference signature and its identification over land and ocean," *IEEE Trans. Geosci. Rem. Sens.*, vol. 44, pp. 530-539, 2006.